Revealing QCD thermodynamics in ultrarelativistic nuclear collisions

Fernando G. Gardim,[1,2] Giuliano Giacalone,[2] Matthew Luzum,[3] and Jean-Yves Ollitrault[2]

[1] *Instituto de Ciência e Tecnologia, Universidade Federal de Alfenas, 37715-400 Poços de Caldas, MG, Brazil*
[2] *Institut de physique théorique, Université Paris Saclay, CNRS, CEA, F-91191 Gif-sur-Yvette, France*
[3] *Instituto de Física, Universidade de São Paulo, R. do Matão 1371, 05508-090 São Paulo, SP, Brazil*

We show that the mean transverse momentum of charged hadrons, $\langle p_t \rangle$, in ultrarelativistic heavy-ion collisions is proportional the temperature of the quark-gluon plasma from which particles are emitted. We introduce an effective hydrodynamic description of the system created in a relativistic heavy-ion collision to relate experimental data on $\langle p_t \rangle$ and charged-particle multiplicity to the thermodynamic properties of the quark-gluon plasma created in experiments. We find that Large Hadron Collider (LHC) data on Pb-Pb collisions at $\sqrt{s_{\rm NN}} = 5.02$ TeV is compatible with a deconfined medium with entropy density $s = 20 \pm 5$ fm^{-3} and speed of sound $c_s^2 = 0.24 \pm 0.04$ at a temperature $T = 222 \pm 9$ MeV, in agreement with lattice calculations. We identify the main sources of theoretical error in the extraction of these quantities from heavy-ion data.

The hydrodynamic framework of heavy-ion collisions successfully explains the bulk of particle production. The little droplet of quark-gluon plasma undergoes a very quick phase of thermalization [1] before evolving according to the equations of relativistic hydrodynamics [2]. The fluid eventually decouples into individual particles as its density decreases [3]. This freeze-out yields a number of resonances which decay into stable hadrons [4, 5].

The relation between the temperature of the medium in the hydrodynamic phase and the mean transverse momentum of unidentified charged hadrons, $\langle p_t \rangle$, has been speculated for decades [6, 7]. However, despite early attempts [8, 9], it has never been explored in the context of hydrodynamic simulations. The reason is that the temperature of the quark-gluon plasma is not a single number, but a nontrivial function of space and time. In this paper we introduce an effective temperature, $T_{\rm eff}$, which averages out this complex space-time information, and which follows closely the $\langle p_t \rangle$ of charged particles, irrespective of collision centrality, colliding species, center-of-mass energy, and viscous corrections. We argue that the dependence of $\langle p_t \rangle$ on collision energy provides a robust measure of the speed of sound of the quark-gluon plasma produced in these collisions.

We define the effective temperature, $T_{\rm eff}$, and the effective volume, $V_{\rm eff}$, of the quark-gluon plasma as those of a uniform fluid at rest which would have the same energy, E, and entropy, S, as the fluid at freeze-out. They are defined by the equations

$$\begin{aligned} E &= \int_{\rm f.o.} T^{0\mu} d\sigma_\mu = \epsilon(T_{\rm eff}) V_{\rm eff}, \\ S &= \int_{\rm f.o.} s u^\mu d\sigma_\mu = s(T_{\rm eff}) V_{\rm eff}, \end{aligned} \tag{1}$$

where the integrals run over the freeze-out hypersurface. $T^{\mu\nu}$ denotes the stress-energy tensor of the fluid and u^μ the fluid 4-velocity. ϵ and s denote the energy and entropy density in the fluid rest frame, which are related to the temperature T through the equation of state.

By taking the ratio E/S, one eliminates $V_{\rm eff}$, and one can solve the resulting equation for $T_{\rm eff}$, using the equation of state. As will be shown below, $T_{\rm eff}$ and $V_{\rm eff}$ are remarkably independent of the freeze-out temperature. Hence, they provide simple and unambiguous measures of the thermodynamic state of the fluid, averaged over its space-time history.

Before embarking on quantitative calculations, let us draw a simple picture of how these quantities are related to observables. In thermodynamics, the energy per particle is typically proportional to the temperature. Specifically, it is equal to $3T$ in a massless ideal gas with Boltzmann statistics [10]. The transverse momentum of a particle concides with its energy in the ultrarelativistic limit and near midrapidity. Therefore, it is natural to expect that $\langle p_t \rangle \sim 3T_{\rm eff}$. Furthermore, for a given $T_{\rm eff}$, one expects the charged multiplicity per unit pseudorapidity $dN_{\rm ch}/d\eta$ to be proportional to the volume $V_{\rm eff}$, since the multiplicity is proportional to the total entropy.

To illustrate and verify this picture, we compute $T_{\rm eff}$ and $V_{\rm eff}$ in hydrodynamic simulations of Pb-Pb collisions. We assume a boost-invariant longitudinal expansion [11], and we neglect the baryon chemical potential. These are good approximations at ultrarelativistic energies. We initialize hydrodynamics at a time $\tau_0 = 0.6$ fm/c [12] after the collision. We neglect the transverse expansion before τ_0 [13–15]. We assume that the entropy density at time τ_0 at a given transverse point $\mathbf{r}$, $s(\tau_0, \mathbf{r})$, is proportional to $\sqrt{T_A T_B}$ computed at $\mathbf{r}$ [16, 17], where A and B label the two colliding nuclei, and $T_{A/B}$ is the integral of the nuclear density along the longitudinal coordinate (or, equivalently, the thickness function in the optical Glauber model [18]). The proportionality factor is adjusted at each collision centrality so as to match the observed charged multiplicity near midrapidity [19, 20].

The centrality is specified by the impact parameter, b, of the collision. The relation between centrality fraction, c, and the impact parameter is geometric, $c = \pi b^2/\sigma_{\rm PbPb}$, $\sigma_{\rm PbPb} = 767$ fm^2 being the total inelastic cross section of Pb-Pb collisions at $\sqrt{s_{\rm NN}} = 5.02$ TeV [21]. We run a single hydrodynamic event at each centrality.

The choice of taking $\sqrt{T_A T_B}$ is motivated by the phenomenological success of the T_RENTo model of initial

conditions [22], where the same prescription for entropy deposition is used, although with the inclusion of initial-state fluctuations [23]. We include initial-state fluctuations in our smooth calculation through their effect on the transverse size of the system. The mean transverse momentum in hydrodynamics is sensitive to the transverse size [24], which is somewhat reduced by initial state fluctuations. To take into account this reduction, at each impact parameter we shrink our smooth initial conditions so that they present the same radius R_0 (see below Eq. (2)) as in the full T_RENTo parametrization, tuned to data as in Ref. [25]. The correction to the size is of order 5%, 15%, 30% at $b = 2$, 7, 12 fm, respectively.

The fluctuation-corrected initial conditions are then evolved using the MUSIC hydrodynamic code [26–28]. We run ideal and viscous hydrodynamic simulations. In order to assess separately the effects of shear and bulk viscosity, we implement either a constant shear viscosity over entropy ratio, $\eta/s = 0.2$ [29, 30], or a bulk viscosity parametrized as in Ref. [31]. Cooper-Frye freeze-out [32] is implemented at the temperature $T_{\rm f.o.} = 156.5$ MeV [33], a reasonable choice in a hydrodynamic setup that does not implement partial chemical equilibrium [29, 34–36] or a hadronic cascade [37, 38]. The viscous corrections to the momentum distribution functions are evaluated using the quadratic ansatz [39–41]. We take into account hadronic decays after freeze-out, but we neglect rescatterings in the hadronic phase [31, 42, 43].

We evaluate the mean transverse momentum of charged hadrons in the pseudorapidity interval $|\eta| < 0.8$. This observable does not require particle identification, unlike the mean transverse mass [44–46], but it requires to cover the whole p_t range, and the low p_t particles are not detected. There are two strategies in order to compare theory and experiment: One can either implement the same p_t cut in the calculation, or extrapolate experimental data down to $p_t = 0$. We choose the latter approach, because hydrodynamics is meant to describe the bulk of particle production, and because this extrapolation has been carried out by some of the experiments.

Figure 1 (a) displays the centrality dependence of $\langle p_t \rangle$ and $T_{\rm eff}$ in Pb+Pb collisions at $\sqrt{s_{\rm NN}} = 5.02$ TeV. The proportionality relation $\langle p_t \rangle = 3.07\ T_{\rm eff}$ is satisfied to an excellent accuracy across the full range of centrality, confirming the expectation $\langle p_t \rangle \sim 3T_{\rm eff}$. Shear viscosity increases $\langle p_t \rangle$ while bulk viscosity decreases it [49]. The remarkable result is that $T_{\rm eff}$ is modified by the same relative amount, so that $\langle p_t \rangle = 3.07\ T_{\rm eff}$ holds irrespective of transport coefficients. Note that hydrodynamics captures both the absolute magnitude and the centrality dependence [30] of experimental data [47], shown as symbols in Fig. 1 (a). The experimental observation that $\langle p_t \rangle$ is almost independent of centrality implies in turn that different centralities correspond to the same $T_{\rm eff}$.

Figure 1 (c) displays the variation of $V_{\rm eff}$ with centrality. This volume is mainly determined by the initial density profile. We define the initial radius, R_0, as

$$(R_0)^2 \equiv \frac{2\int_{\mathbf{r}} |\mathbf{r}|^2 s(\tau_0, \mathbf{r})}{\int_{\mathbf{r}} s(\tau_0, \mathbf{r})}, \tag{2}$$

where $s(\tau_0, \mathbf{r})$ is the entropy density and the integration runs over the transverse plane. The factor 2 in the numerator ensures that for a uniform density profile in a circle of radius R_0, the right-hand side gives $(R_0)^2$. For dimensional reasons, the duration of longitudinal cooling is proportional to R_0, and the volume $V_{\rm eff}$ is proportional to $(R_0)^3$. This is confirmed by the results in Fig. 1 (c): In ideal hydrodynamics, $V_{\rm eff}$ is the volume of a cylinder of base area πR_0^2 and height $\sim 1.2R_0$ for all centralities. This implies that two hydrodynamic calculations with the same particle density per unit volume $(1/R_0^3)dN_{\rm ch}/d\eta$ will also have the same $T_{\rm eff}$ and $\langle p_t \rangle$. Note also that the variation of $V_{\rm eff}$ with centrality closely follows that of the charged multiplicity, $dN_{\rm ch}/d\eta$.

We now study the dependence of $\langle p_t \rangle$ on system size. Figure 2 displays a comparison between hydrodynamic simulations of Xe-Xe collisions at $\sqrt{s_{\rm NN}} = 5.44$ TeV and Pb-Pb collisions at $\sqrt{s_{\rm NN}} = 5.02$ TeV. We only run ideal hydrodynamics for this comparison. Values of $\langle p_t \rangle$ and $T_{\rm eff}$ are almost identical for both systems. This robust prediction of hydrodynamics [25] is confirmed by experimental data. Once scaled by the mass number A, the charged multiplicity and the effective volume are identical for both systems [50] (Fig. 2 (b)).

We now look at the dependence on collision energy of $T_{\rm eff}$ and $\langle p_t \rangle$ for central Pb+Pb collisions. Figures 1(b) and (d) display the variation of $\langle p_t \rangle$, $T_{\rm eff}$ and $V_{\rm eff}$ as a function of $dN_{\rm ch}/d\eta$ in the window $|\eta| < 0.5$, scaled by the mass number A. This ensures that the plot would be essentially identical for other symmetric collisions, such as Xe+Xe, Cu+Cu or Au+Au [51]. The proportionality between $\langle p_t \rangle$ and $T_{\rm eff}$ holds across a wide range of collision energies, irrespective of transport coefficients. Deviations at the level of few percent appear only at Relativistic Heavy Ion Collider (RHIC) energies. The volume $V_{\rm eff}$ remains essentially constant, which confirms that it is mostly determined by the initial radius, R_0. The slightly larger values at lower energies can be attributed to the softer equation of state, which slows down the expansion.

We conclude that, in hydrodynamic simulations, the ratio of the mean transverse momentum to the effective temperature is independent of transport coefficients, collision centrality, system size, and collision energy, and that the effective volume depends very weakly on the collision energy. These are general properties of hydrodynamic calculations, which should not depend on model details. We now apply these results to evaluate thermodynamic quantities from experimental heavy-ion data.

According to the results in Fig. 1, the effective temperature is related to the mean transverse momentum $\langle p_t \rangle$ by $T_{\rm eff} \simeq \langle p_t \rangle / 3.07$ from the top RHIC to LHC energies, and beyond. In combination with the experimental result

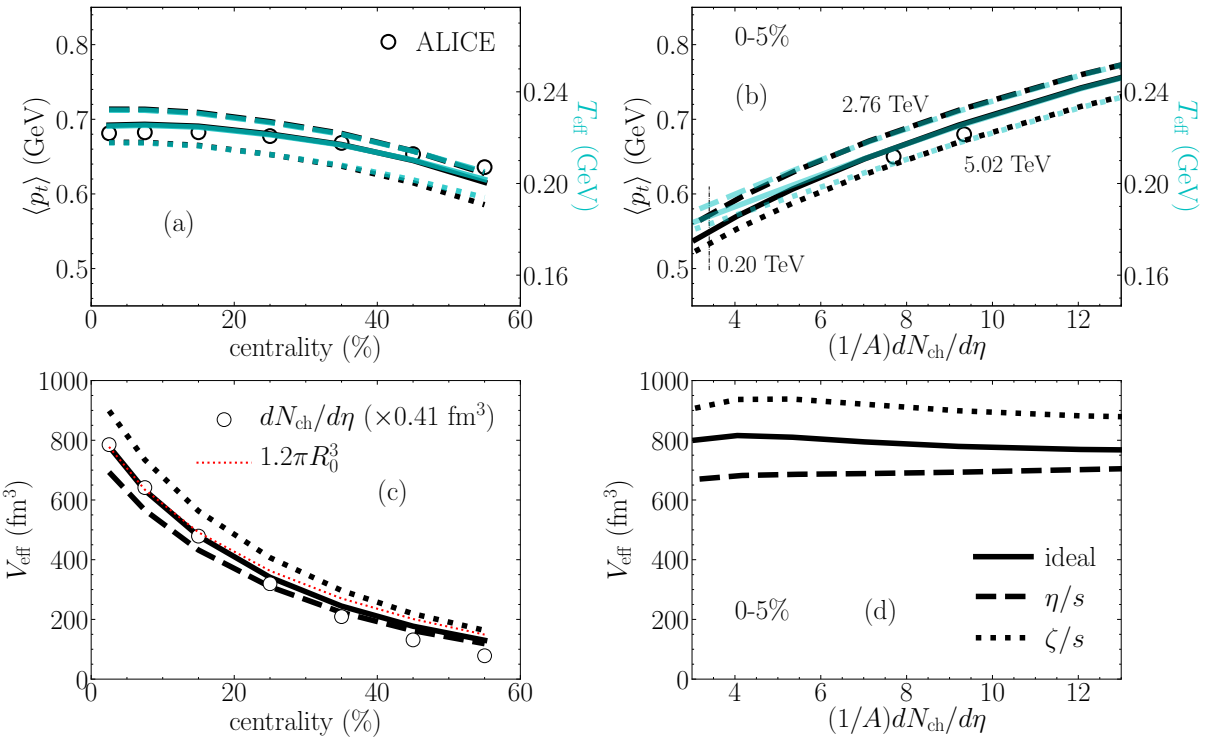

FIG. 1. (a) Centrality dependence of $\langle p_t \rangle$ in Pb-Pb collisions at $\sqrt{s_{\rm NN}} = 5.02$ TeV. Solid, dashed and dotted black lines correspond to ideal hydrodynamics, viscous hydrodynamics with shear viscosity, viscous hydrodynamics with bulk viscosity. Symbols are experimental data [47]. Pale blue lines, which largely overlap with the black lines, correspond to the value of $3.07T_{\rm eff}$. Values of $T_{\rm eff}$ are indicated by the vertical scale on the right. (b) Variation of $\langle p_t \rangle$ and $T_{\rm eff}$ as a function of the charged multiplicity, scaled by the mass number A of the colliding species, for Pb+Pb collsions in the 0-5% centrality window. The experimental value of $(1/A)dN_{\rm ch}/d\eta$ at 200 GeV [48] is indicated as a vertical line. Panels (c) and (d) display the variation of the effective volume $V_{\rm eff}$. Symbols in panel (c) are the experimental values of the charged multiplicity $dN_{\rm ch}/d\eta$ [19], multiplied by 0.41 fm^3, while the dotted line is $1.2\pi R_0^3$, where R_0 is defined by Eq. (2).

$\langle p_t \rangle = 681$ MeV/c [47], we obtain

$$T_{\rm eff} = 222 \pm 9 \text{ MeV} \tag{3}$$

in central Pb+Pb collisions at $\sqrt{s_{\rm NN}} = 5.02$ TeV. The theoretical uncertainty on the value of $T_{\rm eff}$ comes from the proportionality factor between $\langle p_t \rangle$ and $T_{\rm eff}$, which depends on the freeze-out temperature. Thermal fits to particle abundances return a temperature close to 160 MeV [52], which sets a natural upper limit on the freeze-out temperature. On the other hand, any temperature lower than 150 MeV would miss the particle ratios after decays by a significant amount. Figure 3 displays the variation of $T_{\rm eff}$ and $\langle p_t \rangle$ within this range. Note that $T_{\rm eff}$ is significantly higher than $T_{\rm f.o.}$ because $T^{0\mu}$ in Eq. (1) includes the kinetic energy due to the collective motion of the fluid. In fact, $T_{\rm eff}$ is almost *independent* of $T_{\rm f.o.}$, showing a mild increase in Fig. 3, while $\langle p_t \rangle$ decreases. We checked that these results change very little if partial chemical equilibrium is implemented [34]. We conclude that the error on the ratio $\langle p_t \rangle / T_{\rm eff}$ is about 4%, which sets the uncertainty in Eq. (3).

The previous result allows us to perform a back-of-the-envelope estimate of the equation of state. A massless ideal quark-gluon plasma with Boltzmann statistics has a particle density $n = gT^3/\pi^2$ [10], where g is the number of degrees of freedom (color, flavor, spin). If the number of produced hadrons is equal to the number of particles in the quark-gluon plasma, and taking into account that only two thirds of the hadrons are charged, the particle density in the quark-gluon plasma is $n = 1.5(dN_{\rm ch}/d\eta)/V_{\rm eff} \sim 4$ fm^{-3}, where we have used the value of $V_{\rm eff} \approx 780$ fm^3 from Fig. 1(c). With the value of $T_{\rm eff} = 222$ MeV, one obtains $g \sim 30$. This large number shows that the color degrees of freedom are active, or, in other words, that a deconfined state is produced.

We now evaluate the entropy density at $T_{\rm eff}$ from experimental data. The charged multiplicity gives a direct measure of the entropy. A recent evaluation of the entropy per particle from HBT radii and identified particle spectra in Pb+Pb collisions at 2.76 TeV gives $S/N_{\rm ch} = 6.7 \pm 0.8$ [53]. The effective entropy density is then related to the multiplicity through the formula:

$$s(T_{\rm eff}) = \frac{1}{V_{\rm eff}} \frac{S}{N_{\rm ch}} \frac{dN_{\rm ch}}{dy}. \tag{4}$$

The theoretical uncertainty on $V_{\rm eff}$ depends on transport coefficients and initial conditions. The uncertainty due

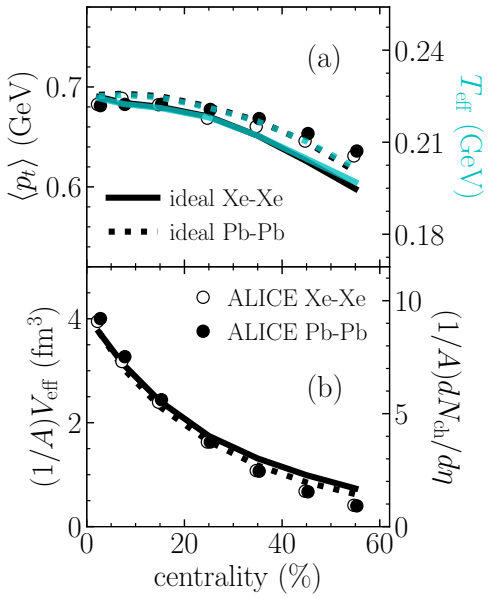

FIG. 2. Comparison between Pb+Pb collisions at $\sqrt{s_{\rm NN}} = 5.02$ TeV and Xe+Xe collisions at $\sqrt{s_{\rm NN}} = 5.44$ TeV. Lines are ideal hydrodynamic calculations. (a) Centrality dependence of $\langle p_t \rangle$ and $T_{\rm eff}$. Symbols are experimental data on $\langle p_t \rangle$ [20, 47]. (b) Centrality dependence of $V_{\rm eff}$ scaled by the mass number A. Symbols: data for $(1/A)dN_{\rm ch}/d\eta$ [19, 20].

to transport coefficients can be evaluated from Fig. 1 (d) and is of the order of 15%. The uncertainty due to the initial size is comparable. Different models of initial conditions give values of R_0 (see Eq. (2)) that differ from the one used in our calculation by up to 3.5%. Since $V_{\rm eff}$ is proportional to R_0^3, this results in a 11% uncertainty on $V_{\rm eff}$. Taking $dN_{\rm ch}/d\eta$ from ALICE data [19] and $V_{\rm eff}$ from the ideal hydrodynamic calculation in Fig. 1 (d), assuming that $dN/dy \simeq 1.15 dN/d\eta$ near midrapidity [53], and adding all errors in quadrature, we obtain, at $\sqrt{s_{\rm NN}} = 5.02$ TeV,

$$s(T_{\rm eff}) = 20 \pm 5 \ {\rm fm}^{-3}. \qquad (5)$$

This estimate can be compared with theoretical calculations of the equation of state in lattice QCD. With realistic quark masses [54], these calculations give $s_{\rm QCD}(T = 222) \simeq 17$ fm^{-3}, in agreement with our estimate.

Quite remarkably, all large sources of uncertainty (freeze-out temperature, transport coefficients, system size) cancel if one considers the relative variation of $\langle p_t \rangle$ and $dN_{\rm ch}/d\eta$ with colliding energy, rather than their absolute values. The effective volume is essentially constant with energy, so that the effective entropy density is proportional to the multiplicity; Analogously, the effective temperature is proportional to $\langle p_t \rangle$. This implies:

$$\frac{ds(T_{\rm eff})}{s(T_{\rm eff})} = \frac{dN_{\rm ch}}{N_{\rm ch}}, \qquad \frac{dT_{\rm eff}}{T_{\rm eff}} = \frac{d\langle p_t \rangle}{\langle p_t \rangle}. \qquad (6)$$

These relative variations do not involve the proportionality coefficients, which are the dominant error for both

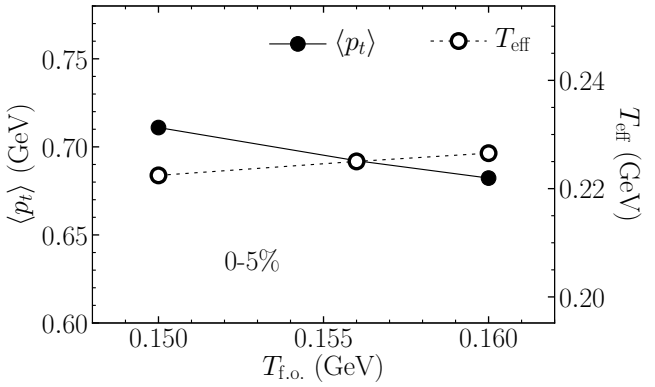

FIG. 3. Variation of $\langle p_t \rangle$ and $T_{\rm eff}$ as a function of the freeze-out temperature in ideal hydrodynamic simulations of central Pb+Pb collisions at $\sqrt{s_{\rm NN}} = 5.02$ TeV.

quantities. Taking the ratio of the right-hand sides in Eq. (6), one obtains the velocity of sound at $T_{\rm eff}$:

$$c_s^2(T_{\rm eff}) \equiv \frac{dP}{d\varepsilon} = \left.\frac{sdT}{Tds}\right|_{T_{\rm eff}} = \frac{d\ln\langle p_t \rangle}{d\ln(dN_{\rm ch}/d\eta)}. \qquad (7)$$

We estimate the right-hand side using 0-5% central Pb-Pb data. We use the extrapolated values of $dN_{\rm ch}/d\eta$ at 2.76 TeV [55] and 5.02 TeV [19], and p_t spectra from Ref. [56], without carrying any extrapolation down to $p_t = 0$, i.e., assuming that the relative variation of $\langle p_t \rangle$ is insensitive to the extrapolation. We obtain

$$c_s^2(T_{\rm eff}) = 0.24 \pm 0.04, \qquad (8)$$

where the error bar comes from taking into account the possible variation of the effective volume between the two energies, which we estimate to be at most 3% according to the results in Fig. 1 (d). Our result in Eq. (8) is in agreement with the lattice value $c_s^2 = 0.252$ at $T = 222$ MeV [54]. Since we use data from the same detector, it is likely that experimental errors also cancel to a large extent as one studies variation with $\sqrt{s}$. Note that Eq. (7) explains the conclusion from the Bayesian analysis of Ref. [57], that the RHIC and LHC data in combination provide a better constraint on the speed of sound than either alone. We do not show RHIC data for the following reason: The latest data on spectra [58] are limited to $p_t > 0.5$ GeV, and the extrapolation down to $p_t = 0$ would entail large errors.

In summary, we have introduced a simple effective description of the system created in heavy-ion collisions. Combined with hydrodynamic simulations, it allows us to infer the thermodynamic properties of the quark-gluon plasma created in experiments, and could be used to perform comparisons between the results of different hydrodynamic models. Our study could be generalized to include nonzero baryon chemical potential at lower energies. A proper treatment of fluctuations may also lead to new insight, since the fluctuations of $\langle p_t \rangle$ [59–61] should be determined mostly by the fluctuations of $T_{\rm eff}$.

ACKNOWLEDGMENTS

F.G.G. was supported by Conselho Nacional de Desenvolvimento Científico e Tecnológico (CNPq grant 205369/2018-9 and 312932/2018-9) and FAPEMIG (grant APQ-02107-16. M.L. acknowledges support from FAPESP projects 2016/24029-6 and 2017/05685-2. F.G.G. and M.L. acknowledge support from project INCT-FNA Proc. No. 464898/2014-5 and G.G., M.L. and J.-Y.O. from USP-COFECUB (grant Uc Ph 160-16, 2015/13).

[1] S. Schlichting and D. Teaney, arXiv:1908.02113 [nucl-th].

[2] P. Romatschke and U. Romatschke, doi:10.1017/9781108651998 arXiv:1712.05815 [nucl-th].

[3] W. Broniowski and W. Florkowski, Phys. Rev. Lett. **87**, 272302 (2001) doi:10.1103/PhysRevLett.87.272302 [nucl-th/0106050].

[4] P. Alba, V. Mantovani Sarti, J. Noronha, J. Noronha-Hostler, P. Parotto, I. Portillo Vazquez and C. Ratti, Phys. Rev. C **98**, no. 3, 034909 (2018) doi:10.1103/PhysRevC.98.034909 [arXiv:1711.05207 [nucl-th]].

[5] A. Mazeliauskas, S. Floerchinger, E. Grossi and D. Teaney, Eur. Phys. J. C **79**, no. 3, 284 (2019) doi:10.1140/epjc/s10052-019-6791-7 [arXiv:1809.11049 [nucl-th]].

[6] L. Van Hove, Phys. Lett. B **118**, 138 (1982) [Phys. Lett. **118B**, 138 (1982)]. doi:10.1016/0370-2693(82)90617-7

[7] R. Campanini, G. Ferri and G. Ferri, Phys. Lett. B **703**, 237 (2011) doi:10.1016/j.physletb.2011.08.009 [arXiv:1106.2008 [hep-ph]].

[8] L. D. McLerran, M. Kataja, P. V. Ruuskanen and H. von Gersdorff, Phys. Rev. D **34**, 2755 (1986). doi:10.1103/PhysRevD.34.2755

[9] J. P. Blaizot and J. Y. Ollitrault, Phys. Lett. B **191**, 21 (1987). doi:10.1016/0370-2693(87)91314-1

[10] J. Y. Ollitrault, Eur. J. Phys. **29**, 275 (2008) doi:10.1088/0143-0807/29/2/010 [arXiv:0708.2433 [nucl-th]].

[11] J. D. Bjorken, Phys. Rev. D **27**, 140 (1983). doi:10.1103/PhysRevD.27.140

[12] P. F. Kolb and U. W. Heinz, In *Hwa, R.C. (ed.) et al.: Quark gluon plasma* 634-714 [nucl-th/0305084].

[13] J. Vredevoogd and S. Pratt, Phys. Rev. C **79**, 044915 (2009) doi:10.1103/PhysRevC.79.044915 [arXiv:0810.4325 [nucl-th]].

[14] W. van der Schee, P. Romatschke and S. Pratt, Phys. Rev. Lett. **111**, no. 22, 222302 (2013) doi:10.1103/PhysRevLett.111.222302 [arXiv:1307.2539 [nucl-th]].

[15] L. Keegan, A. Kurkela, A. Mazeliauskas and D. Teaney, JHEP **1608**, 171 (2016) doi:10.1007/JHEP08(2016)171 [arXiv:1605.04287 [hep-ph]].

[16] K. J. Eskola, K. Kajantie and K. Tuominen, Phys. Lett. B **497**, 39 (2001) doi:10.1016/S0370-2693(00)01341-1 [hep-ph/0009246].

[17] P. F. Kolb, U. W. Heinz, P. Huovinen, K. J. Eskola and K. Tuominen, Nucl. Phys. A **696**, 197 (2001) doi:10.1016/S0375-9474(01)01114-9 [hep-ph/0103234].

[18] M. L. Miller, K. Reygers, S. J. Sanders and P. Steinberg, Ann. Rev. Nucl. Part. Sci. **57**, 205 (2007) doi:10.1146/annurev.nucl.57.090506.123020 [nucl-ex/0701025].

[19] J. Adam *et al.* [ALICE Collaboration], Phys. Rev. Lett. **116**, no. 22, 222302 (2016) doi:10.1103/PhysRevLett.116.222302 [arXiv:1512.06104 [nucl-ex]].

[20] S. Acharya *et al.* [ALICE Collaboration], Phys. Lett. B **790**, 35 (2019) doi:10.1016/j.physletb.2018.12.048 [arXiv:1805.04432 [nucl-ex]].

[21] B. Abelev *et al.* [ALICE Collaboration], Phys. Rev. C **88**, no. 4, 044909 (2013) doi:10.1103/PhysRevC.88.044909 [arXiv:1301.4361 [nucl-ex]].

[22] J. S. Moreland, J. E. Bernhard and S. A. Bass, Phys. Rev. C **92**, no. 1, 011901 (2015) doi:10.1103/PhysRevC.92.011901 [arXiv:1412.4708 [nucl-th]].

[23] Y. Hama, T. Kodama and O. Socolowski, Jr., Braz. J. Phys. **35**, 24 (2005) doi:10.1590/S0103-97332005000100003 [hep-ph/0407264].

[24] W. Broniowski, M. Chojnacki and L. Obara, Phys. Rev. C **80**, 051902 (2009) doi:10.1103/PhysRevC.80.051902 [arXiv:0907.3216 [nucl-th]].

[25] G. Giacalone, J. Noronha-Hostler, M. Luzum and J. Y. Ollitrault, Phys. Rev. C **97**, no. 3, 034904 (2018) doi:10.1103/PhysRevC.97.034904 [arXiv:1711.08499 [nucl-th]].

[26] B. Schenke, S. Jeon and C. Gale, Phys. Rev. C **82**, 014903 (2010) doi:10.1103/PhysRevC.82.014903 [arXiv:1004.1408 [hep-ph]].

[27] B. Schenke, S. Jeon and C. Gale, Phys. Rev. C **85**, 024901 (2012) doi:10.1103/PhysRevC.85.024901 [arXiv:1109.6289 [hep-ph]].

[28] J. F. Paquet, C. Shen, G. S. Denicol, M. Luzum, B. Schenke, S. Jeon and C. Gale, Phys. Rev. C **93**, no. 4, 044906 (2016) doi:10.1103/PhysRevC.93.044906 [arXiv:1509.06738 [hep-ph]].

[29] U. Heinz and R. Snellings, Ann. Rev. Nucl. Part. Sci. **63**, 123 (2013) doi:10.1146/annurev-nucl-102212-170540 [arXiv:1301.2826 [nucl-th]].

[30] H. Niemi, K. J. Eskola and R. Paatelainen, Phys. Rev. C **93**, no. 2, 024907 (2016) doi:10.1103/PhysRevC.93.024907 [arXiv:1505.02677 [hep-ph]].

[31] J. E. Bernhard, J. S. Moreland, S. A. Bass, J. Liu and U. Heinz, Phys. Rev. C **94**, no. 2, 024907 (2016) doi:10.1103/PhysRevC.94.024907 [arXiv:1605.03954 [nucl-th]].

[32] F. Cooper and G. Frye, Phys. Rev. D **10**, 186 (1974). doi:10.1103/PhysRevD.10.186

[33] P. Huovinen and P. V. Ruuskanen, Ann. Rev. Nucl. Part. Sci. **56**, 163 (2006) doi:10.1146/annurev.nucl.54.070103.181236 [nucl-th/0605008].

[34] P. Huovinen and P. Petreczky, Nucl. Phys. A **837**, 26 (2010) doi:10.1016/j.nuclphysa.2010.02.015

[arXiv:0912.2541 [hep-ph]].
[35] C. Gale, S. Jeon, B. Schenke, P. Tribedy and R. Venugopalan, Phys. Rev. Lett. **110**, no. 1, 012302 (2013) doi:10.1103/PhysRevLett.110.012302 [arXiv:1209.6330 [nucl-th]].
[36] K. J. Eskola, H. Niemi, R. Paatelainen and K. Tuominen, Phys. Rev. C **97**, no. 3, 034911 (2018) doi:10.1103/PhysRevC.97.034911 [arXiv:1711.09803 [hep-ph]].
[37] R. D. Weller and P. Romatschke, Phys. Lett. B **774**, 351 (2017) doi:10.1016/j.physletb.2017.09.077 [arXiv:1701.07145 [nucl-th]].
[38] A. Dubla, S. Masciocchi, J. M. Pawlowski, B. Schenke, C. Shen and J. Stachel, Nucl. Phys. A **979**, 251 (2018) doi:10.1016/j.nuclphysa.2018.09.046 [arXiv:1805.02985 [nucl-th]].
[39] D. Teaney, Phys. Rev. C **68**, 034913 (2003) doi:10.1103/PhysRevC.68.034913 [nucl-th/0301099].
[40] K. Dusling, G. D. Moore and D. Teaney, Phys. Rev. C **81**, 034907 (2010) doi:10.1103/PhysRevC.81.034907 [arXiv:0909.0754 [nucl-th]].
[41] P. Bozek, Phys. Rev. C **81**, 034909 (2010) doi:10.1103/PhysRevC.81.034909 [arXiv:0911.2397 [nucl-th]].
[42] D. Teaney, J. Lauret and E. V. Shuryak, Phys. Rev. Lett. **86**, 4783 (2001) doi:10.1103/PhysRevLett.86.4783 [nucl-th/0011058].
[43] H. Petersen, J. Steinheimer, G. Burau, M. Bleicher and H. Stocker, Phys. Rev. C **78**, 044901 (2008) doi:10.1103/PhysRevC.78.044901 [arXiv:0806.1695 [nucl-th]].
[44] H. Petersen, J. Steinheimer, M. Bleicher and H. Stocker, J. Phys. G **36**, 055104 (2009) doi:10.1088/0954-3899/36/5/055104 [arXiv:0902.4866 [nucl-th]].
[45] X. Luo, Nucl. Phys. A **956**, 75 (2016) doi:10.1016/j.nuclphysa.2016.03.025 [arXiv:1512.09215 [nucl-ex]].
[46] A. Monnai and J. Y. Ollitrault, Phys. Rev. C **96**, no. 4, 044902 (2017) doi:10.1103/PhysRevC.96.044902 [arXiv:1707.08466 [nucl-th]].
[47] S. Acharya *et al.* [ALICE Collaboration], Phys. Lett. B **788**, 166 (2019) doi:10.1016/j.physletb.2018.10.052 [arXiv:1805.04399 [nucl-ex]].
[48] B. B. Back *et al.* [PHOBOS Collaboration], Phys. Rev. C **65**, 061901 (2002) doi:10.1103/PhysRevC.65.061901 [nucl-ex/0201005].
[49] A. Monnai and T. Hirano, Phys. Rev. C **80**, 054906 (2009) doi:10.1103/PhysRevC.80.054906 [arXiv:0903.4436 [nucl-th]].
[50] R. Rogly, G. Giacalone and J. Y. Ollitrault, Nucl. Phys. A **982**, 355 (2019) doi:10.1016/j.nuclphysa.2018.10.071 [arXiv:1807.07831 [nucl-th]].
[51] G. Giacalone, A. Mazeliauskas and S. Schlichting, arXiv:1908.02866 [hep-ph].
[52] A. Andronic, P. Braun-Munzinger, K. Redlich and J. Stachel, Nature **561**, no. 7723, 321 (2018) doi:10.1038/s41586-018-0491-6 [arXiv:1710.09425 [nucl-th]].
[53] P. Hanus, A. Mazeliauskas and K. Reygers, arXiv:1908.02792 [hep-ph].
[54] S. Borsanyi, Z. Fodor, C. Hoelbling, S. D. Katz, S. Krieg and K. K. Szabo, Phys. Lett. B **730**, 99 (2014) doi:10.1016/j.physletb.2014.01.007 [arXiv:1309.5258 [hep-lat]].
[55] K. Aamodt *et al.* [ALICE Collaboration], Phys. Rev. Lett. **106**, 032301 (2011) doi:10.1103/PhysRevLett.106.032301 [arXiv:1012.1657 [nucl-ex]].
[56] S. Acharya *et al.* [ALICE Collaboration], JHEP **1811**, 013 (2018) doi:10.1007/JHEP11(2018)013 [arXiv:1802.09145 [nucl-ex]].
[57] S. Pratt, E. Sangaline, P. Sorensen and H. Wang, Phys. Rev. Lett. **114**, 202301 (2015) doi:10.1103/PhysRevLett.114.202301 [arXiv:1501.04042 [nucl-th]].
[58] A. Adare *et al.* [PHENIX Collaboration], Phys. Rev. C **88**, no. 2, 024906 (2013) doi:10.1103/PhysRevC.88.024906 [arXiv:1304.3410 [nucl-ex]].
[59] J. Adams *et al.* [STAR Collaboration], Phys. Rev. C **71**, 064906 (2005) doi:10.1103/PhysRevC.71.064906 [nucl-ex/0308033].
[60] P. Bozek and W. Broniowski, Phys. Rev. C **85**, 044910 (2012) doi:10.1103/PhysRevC.85.044910 [arXiv:1203.1810 [nucl-th]].
[61] B. B. Abelev *et al.* [ALICE Collaboration], Eur. Phys. J. C **74**, no. 10, 3077 (2014) doi:10.1140/epjc/s10052-014-3077-y [arXiv:1407.5530 [nucl-ex]].